Magnetic Resonance in Medicine 60:510–516 (2008)

Evaluation of Lactate and Alanine as Metabolic Biomarkers of Prostate Cancer Using ^{1}H HR-MAS Spectroscopy of Biopsy Tissues

May-Britt Tessem,[1,4] Mark G. Swanson,[1] Kayvan R. Keshari,[1] Mark J. Albers,[1] David Joun,[1] Z. Laura Tabatabai,[2,3] Jeffry P. Simko,[2] Katsuto Shinohara,[4] Sarah J. Nelson,[1] Daniel B. Vigneron,[1] Ingrid S. Gribbestad,[5] and John Kurhanewicz[1,4]*

The goal of this study was to investigate the use of lactate and alanine as metabolic biomarkers of prostate cancer using ^{1}H high-resolution magic angle spinning (HR-MAS) spectroscopy of snap-frozen transrectal ultrasound (TRUS)-guided prostate biopsy tissues. A long-echo-time rotor-synchronized Carr-Purcell-Meiboom-Gill (CPMG) sequence including an electronic reference to access in vivo concentrations (ERETIC) standard was used to determine the concentrations of lactate and alanine in 82 benign and 16 malignant biopsies (mean 26.5% ± 17.2% of core). Low concentrations of lactate (0.61 ± 0.28 mmol/kg) and alanine (0.14 ± 0.06 mmol/kg) were observed in benign prostate biopsies, and there was no significant difference between benign predominantly glandular (N = 54) and stromal (N = 28) biopsies between patients with (N = 38) and without (N = 44) a positive clinical biopsy. In biopsies containing prostate cancer there was a highly significant (P < 0.0001) increase in lactate (1.59 ± 0.61 mmol/kg) and alanine (0.26 ± 0.07 mmol/kg), and minimal overlap with lactate concentrations in benign biopsies. This study demonstrates for the first time very low concentrations of lactate and alanine in benign prostate biopsy tissues. The significant increase in the concentration of both lactate and alanine in biopsy tissue containing as little as 5% cancer could be exploited in hyperpolarized ^{13}C spectroscopic imaging (SI) studies of prostate cancer patients. Magn Reson Med 60:510–516, 2008. © 2008 Wiley-Liss, Inc.

Key words: lactate; alanine; HR-MAS; ERETIC; hyperpolarized ^{13}C

Combined MRI and three-dimensional MR spectroscopic imaging (MRI/3D-MRSI) studies of prostate cancer patients have been shown to significantly improve the clinical localization of cancer within the prostate (1–6), improve the prediction of extracapsular extension (ECE) (7,8), and provide a measure of prostate cancer aggressiveness (9,10) and therapeutic response (11–13). However, with the widespread use of serum prostate-specific antigen (PSA) screening and systematic transrectal ultrasound (TRUS)-guided biopsies, there has been an increase in early detection and a significant downstaging of prostate cancer in recent years (14,15). Consequently, there is a growing need for additional biomarkers and multiparametric imaging approaches that can predict the metastatic potential of early-stage cancers and be used to monitor patients during active surveillance, conventional therapies, and clinical trials of emerging therapies.

While the current commercially available clinical MRI/MRSI prostate exam relies on changes in choline, citrate, and polyamine metabolism, lactate and alanine have largely been ignored due to the difficulty of suppressing the large signals from overlapping periprostatic lipids (16). New hyperpolarized ^{13}C MRS techniques (17–19) and advances in lipid suppression and spectral edited ^{1}H MRS (20,21) provide the opportunity to observe changes in lactate and alanine in clinical MRI/MRSI exams. Studies in the transgenic adenocarcinoma of mouse prostate (TRAMP) (22) model of prostate cancer have demonstrated >50,000-fold polarization enhancements of ^{13}C pyruvate, providing a sufficient signal-to-noise ratio (SNR) for high spatial and temporal resolution ^{13}C MRS of the metabolic products lactate and alanine from regions of primary and metastatic prostate cancer (18). These studies demonstrated a significant pathologic grade-dependent increase in lactate in this murine model of prostate cancer.

Previous biochemical (23) and ^{1}H spectroscopic studies of tissue extracts (24–26), and more recent ^{1}H high-resolution magic angle spinning (HR-MAS) spectroscopy studies (27) of intact tissues have reported inconsistent changes in lactate and/or alanine in prostate cancer vs. benign prostate tissues. These discrepancies could arise from both the different experimental methods and sources of tissue used, i.e., postsurgical, transurethral resection (TURP), or biopsy. Postsurgical prostate tissues are acquired in an unknown state of metabolic degradation because the prostate can be removed from its blood supply

[1]Department of Radiology, University of California–San Francisco, San Francisco, California, USA.

[2]Department of Pathology, University of California–San Francisco, San Francisco, California, USA.

[3]Veterans Administration Medical Center, San Francisco, California, USA.

[4]Department of Urology, University of California–San Francisco, San Francisco, California, USA.

[5]Department of Circulation and Medical Imaging, Norwegian University of Science and Technology, Trondheim, Norway.

Grant sponsor: National Institutes of Health; Grant numbers: R21 EB05363, R01 CA102751, K01 CA96618; Grant sponsor: American Cancer Society; Grant number: RSG-05-241-01-CCE; Grant sponsor: University of California; Grant numbers: LSIT01-10107, ITL-BIO04-10148.

*Correspondence to: John Kurhanewicz, Ph.D., Professor of Radiology, Urology and Pharmaceutical Chemistry, Byers Hall, Room 203E, 1700 4th Street, San Francisco, CA 94158-2330. E-mail: John.Kurhanewicz@radiology.ucsf.edu

Received 13 September 2007; revised 4 April 2008; accepted 23 April 2008.

DOI 10.1002/mrm.21694

Published online in Wiley InterScience (www.interscience.wiley.com).

for ≥3 h prior to tissue harvesting. During this period of ischemia, significant anaerobic glycolysis can occur, dramatically affecting the concentrations of glucose, alanine, and lactate (27). Since biopsy tissues can be harvested and frozen in seconds, they provide a more accurate ex vivo "snapshot" of in vivo lactate and alanine metabolism. In this study, quantitative ^{1}H HR-MAS spectroscopy, using the electronic reference to access in vivo concentrations (ERETIC) method (28,29), was applied to snap-frozen prostate biopsy tissues to determine the concentrations of lactate and alanine prior to pathologic analysis of the same tissues. Lactate and alanine concentrations were compared between biopsies containing benign predominantly glandular and stromal tissues, benign samples in men with and without a positive biopsy result, and biopsies containing ≥5% prostate cancer to establish these metabolites as reliable markers of prostate cancer.

MATERIALS AND METHODS

Human Subjects and the TRUS-Guided Biopsy Procedure

This study was approved by our institutional review board (IRB) and informed consent was obtained from all patients. A total of 130 TRUS-guided prostate biopsies were acquired from 82 previously untreated patients (mean age = 64 ± 10 years [range: 35–83 years]; median PSA = 5.6 ± 18.4 μg/liter [range: 1.6–115.9 μg/liter]). During the biopsy procedure, the patient was placed in the lateral decubitus position and a topical anesthetic (Hurricaine® gel; Beutlich Pharmaceuticals, Waukegan, IL, USA) was applied during the digital rectal examination. A 5.0–7.5 MHz TRUS probe was placed into the rectum, and grayscale and color-Doppler ultrasound images were obtained by an experienced urologist. Then 1% lidocaine (10 ml) was injected into the prostate gland at the lateral edges on each side of the gland from base to apex. Under TRUS guidance, an 8–10 core pattern biopsy was performed using an 18-gauge needle (~15 mm × 1 mm cores) for clinical diagnosis, after which two additional research biopsies were acquired from a hypoechoic region suspicious for cancer and from the contralateral side of the peripheral zone. Biopsies were immediately placed in individual cryovials and snap-frozen on dry ice (≤15 s), and then stored at −80°C and analyzed within 2 weeks of harvesting.

Sample Preparation and ^{1}H HR-MAS Spectroscopy

At sample preparation, ~1 mm of tissue was cut and removed from both ends of the biopsy core to remove periprostatic fat, which was not visually discernible. The trimmed biopsy tissue was weighed (mean = 5.2 ± 1.1 mg) and then transferred into a tared 20-μl leak-proof zirconium HR-MAS rotor containing 3.0 μl of deuterium oxide and 0.75 wt% sodium-3-trimethylsilylpropionate-2,2,3,3-d_4 (D_2O+TSP). The rotor was then assembled and placed into the spectrometer after a handling time of ~2–4 min. ^{1}H HR-MAS spectroscopy was performed at 11.7 T (500 MHz for ^{1}H), 1°C, and a 2250 Hz spin rate using a Varian INOVA NMR spectrometer equipped with a 4-mm gHX nanoprobe (Varian Inc, Palo Alto). Fully relaxed pulse-acquire spectra were acquired with a 2-s presaturation delay, 2-s acquisition time, 40,000 points, 20,000-Hz spectral width, 128 transients, and four steady-state pulses. In addition, a rotor-synchronized Carr-Purcell-Meiboom-Gill (CPMG) (30) spin-echo sequence was used to filter signals from overlapping lipids and macromolecules with the same parameters as above except for a 144- or 288-ms echo time (TE) depending on the magnitude of the lipid peaks; 256 or 512 transients, respectively; and 16 steady-state pulses. To validate the correction factor used for T_2 decay in biopsies, CPMG spectra were also acquired with 72-, 144-, and 288-ms TEs on three surgical tissue samples that contained much higher levels of lactate and alanine.

For quantification of prostate metabolites, a synthetic RF signal (ERETIC) was created using PBox (Varian Inc., Palo Alto, CA, USA) and transmitted during the data acquisition (31). The phase and amplitude of the ERETIC peak were chosen to match other peaks in the spectrum, and the signal was transmitted during acquisition using 0 dB of power, a full width at half height of 3.5 Hz, and an offset frequency equivalent to −0.5 ppm. The ERETIC signal was calibrated weekly using standard solutions of D_2O+TSP, lactate, and alanine. Two-dimensional (2D) total correlation spectroscopy (TOCSY) data were also acquired and used to exclude biopsy samples in which the lactate and alanine peaks were contaminated by resonances due to the anesthetic ointment that were not eliminated by the T_2 filter. The TOCSY spectra were acquired using a rotor synchronized adiabatic (WURST-8) mixing scheme with 1-s presaturation delay, 0.2-s acquisition time, 40-ms mixing time, 24 transients/increment, 20,000 × 6000 Hz spectral width, 4096 × 64 complex points, and time ~1 h (32). A total of 32 out of 130 biopsies were considered unusable due to spectral contamination from lipids and/or topical anesthetic (primarily polyethylene glycol) based on both 1D and 2D spectral findings.

^{1}H HR-MAS Spectroscopy Data Processing and Quantification

Data were processed and displayed offline using ACD Labs 1D and 2D NMR processor (version 9; ACD/Labs, Toronto, Canada). The free induction decays (FIDs) were zero-filled to 65K points, apodized with a 0.5-Hz "matched" exponential filter and Fourier-transformed. Each spectrum was manually phased and baseline-corrected as previously described (27). The 98 spectra used in the analysis demonstrated well-resolved lactate and alanine resonances with no overlapping lipid or other contaminants. Lactate and alanine were quantified from the CPMG experiments by integrating the peak areas and correcting for T_2 decay during the echo delay using previously determined T_2 relaxation times for lactate (0.251 ms) and alanine (0.208 ms) (27) according to Eq. [1]:

$$\tilde{A}_m = A_m e^{(-\tau/T_2)}, \quad [1]$$

where $\tilde{A}_m$ = the metabolite area corrected for T_2, A_m = the area of metabolite, τ = TE, and T_2 = relaxation time of the metabolite. Concentrations were calculated relative to the peak area of the ERETIC signal according to Eq. [2]:

$$\frac{\tilde{A}_m}{A_e} \times [H_e] \times \frac{nH_e}{nH_m} \times \frac{1}{\text{Tissue mass}} = [M], \quad [2]$$

where A_e = the area of ERETIC signal, $[H_e]$ = the standard moles of protons associated with the ERETIC signal in mmol, nH_e = the number of protons of ERETIC ($N = 1$), nH_m = the number of protons corresponding to the lactate and alanine doublets ($N = 3$), tissue mass = mass of the prostate biopsy (kg), and [M] = the metabolite concentration in mmol/kg.

Histopathologic Analysis

Following ^{1}H HR-MAS analysis, biopsy tissues were placed in 25 × 20 × 5 mm^3 cryomolds, frozen in Tissue-Tek® optimal cutting temperature (OCT) tissue embedding medium (Fisher, Pittsburgh, PA, USA) over dry ice, and stored at −80°C. Tissues were sectioned at 5–7-μm intervals and −22°C using a Leica CM1850 cryostat (Leica Microsystems, Wetzlar, Germany), placed on individual histology slides, and stained with hematoxylin and eosin (H&E) using a standard protocol. Typically, three sections were made along the long axis of the biopsy to obtain a complete pathologic assessment of the core, and additional sections were cut for high-molecular-weight keratin staining, if needed to confirm the presence of cancer. Two experienced prostate pathologists reviewed the slides and estimated the percentage of benign glandular epithelium, stroma, prostatic intraepithelial neoplasia (PIN), benign prostatic hyperplasia (BPH), chronic inflammation (prostatitis), and prostate cancer present in each core. The Gleason score of the cancer was also recorded, with 2 (1+1) being the least aggressive and 10 (5+5) being the most aggressive pattern. Average percentages of PIN, chronic inflammation, corpora amylacea (coagulated secretions), and atrophy were also noted in the pathology review, and samples were excluded from the healthy group if the percentage of the confounding factor was greater than 10% of the core area.

Statistics

The metabolite concentrations of lactate and alanine were compared between healthy and cancer tissues using a linear mixed-effects model procedure (33), accounting for repeated measurements from the same patient. The model used lactate and alanine as the dependent variable, disease status as the fixed effect, and individual patient as a random effect. In this way, effects of repeated samples from these patients were removed. Specifically, 12 patients contributed two benign biopsies each, and one patient contributed two cancer biopsies. Data were analyzed using JMP (SAS Institute, 2005, version 6.0) assuming a significance level of $P < 0.05$.

RESULTS

Figure 1 shows representative fully relaxed, water-presaturated ^{1}H HR-MAS spectra and corresponding histopathologic sections (H&E) of (a) benign predominantly glandular tissue (5.1 mg, 40% glandular and 60% stromal tissue) and (b) Gleason 3+3 prostate cancer tissue (5.7 mg, 70% cancer and 30% stromal tissue). The lactate to alanine regions from 144-ms CPMG spectra are shown inset. A spinning rate of 2250 Hz resulted in minimal pathologic degradation, while placing the most prominent side band (that of residual water) at ~0.5 ppm, which is outside of the range of the analyzed metabolites. Similar to what has been previously reported for surgical tissues (27,34,35), benign prostate tissue demonstrated high levels of citrate (doublet of doublets at 2.62 ppm) and the polyamines, spermine, spermidine, and putrescine (complex multiplets at 1.78, 2.10, and 3.11 ppm), which were reduced or absent in cancer spectra. In contrast, the choline-containing metabolites choline (Cho, singlet at 3.21 ppm), phosphocholine (PC, singlet at 3.23 ppm), and glycerophosphocholine (GPC, singlet at 3.24 ppm) were elevated in cancer vs. benign glandular and stromal tissues. Broad lipid and macromolecule resonances overlap the lactate (1.33 ppm) and alanine (1.49 ppm) doublets in the water-presaturated pulse-acquire spectra. These broad components were effectively removed by the CPMG experiments (144 or 288 ms) and the expanded regions show higher levels of lactate and alanine in cancer vs. benign prostate biopsies. Repeat CPMG experiments also showed that lactate and alanine concentrations increased an average of 3.6% ± 9.0% and 0.6% ± 5.7%, at 45 and 80 min, respectively, at 1°C and a 2250 Hz spin rate, indicating minimal change during the course of the HR-MAS experiments.

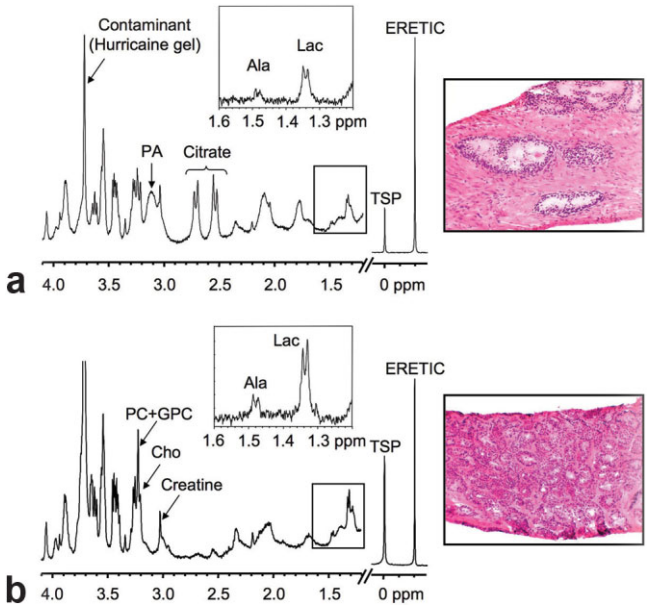

FIG. 1. Representative ^{1}H HR-MAS spectra and corresponding histopathologic sections of (**a**) benign predominantly glandular (40% glandular, 60% stroma) and (**b**) prostate cancer (70% Gleason 3+3) biopsy tissues. The major metabolites, TSP, and ERETIC resonances are shown. Lactate to alanine regions from 144-ms CPMG spectra are shown inset.

On pathology, 82 of the biopsies were benign and 16 contained prostate cancer. The benign samples had on average 21% glandular tissue (ranging from 0% to 40%) and 79% stromal tissue (ranging from 60% to 100%). In the benign group, samples were categorized as 5–10% prostatitis ($N = 7$), 10–30% BPH ($N = 4$), 10% corpora amylacea ($N = 1$), and 10% atrophy ($N = 1$). In cancer tissues the biopsy cores contained an average of 26.5% ± 17.2% cancer (range: 5–80%). The distribution of Gleason

scores was Gleason 3+3 ($N = 10$), 3+4 ($N = 3$), 4+3 ($N = 1$), 4+4 ($N = 1$), and 4+5 ($N = 1$). Since only 6 out of 16 cancer biopsies had a Gleason score greater than 6, it was not possible to determine whether there was a correlation between lactate and/or alanine concentrations and cancer grade. A pathologic review of the clinical and research biopsies indicated that 38 patients had a positive biopsy result (Gleason score: 3+3, 3+4, 4+3, 4+4, 4+5) and 44 patients had no evidence of cancer. A total of 59% of the patients had a prior biopsy, of which 19 patients (23%) were negative and 29 patients (35%) were positive for cancer. All patients with negative clinical biopsies also had negative research biopsies.

There was a highly significant increase in lactate concentrations ($P < 0.0001$) in prostate cancer vs. benign prostate biopsy tissues. Absolute lactate concentrations from benign and malignant prostate biopsy tissues are shown in Fig. 2a. The average lactate concentration was 1.59 ± 0.61 mmol/kg in cancer tissues ($N = 16$) and 0.61 ± 0.28 mmol/kg in benign tissues ($N = 82$). Out of 82 benign biopsies, only 15 samples had individual lactate concentrations overlapping with the concentrations observed in malignant samples. However, the standard deviation (SD) was considerably higher in cancer samples compared to benign samples. Lactate concentrations in benign prostate biopsies were also separated according to whether the biopsy was considered to contain predominantly stromal (>75%) or predominantly glandular tissue (>25%). No significant difference ($P > 0.05$) was observed between lactate levels in benign predominantly stromal (0.61 ± 0.30 mmol/kg, $N = 54$) vs. predominantly glandular (0.61 ± 0.25 mmol/kg, $N = 28$) prostate biopsy tissues.

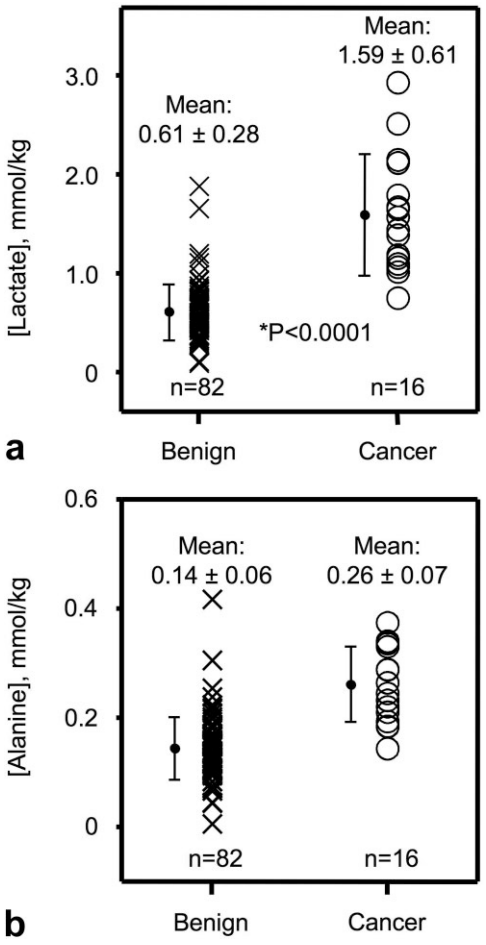

FIG. 2. **a:** Lactate concentrations in benign and malignant prostate biopsy tissues. Minimal overlap (15/82) was observed between benign and cancer tissues. **b:** Alanine concentrations in benign and malignant prostate biopsy tissues. Moderate overlap (39/82) was observed between benign and cancer tissue.

Alanine concentrations ($P < 0.0001$) were also significantly higher in prostate cancer compared to benign tissues. Alanine concentrations from benign and malignant prostate biopsy tissues are shown in Fig. 2b. The average alanine concentration was 0.26 ± 0.07 mmol/kg in malignant samples ($N = 15$) and 0.14 ± 0.06 mmol/kg in benign samples ($N = 82$). The individual alanine concentrations had more overlap between benign and malignant samples than lactate, and the SD in benign tissue was the same as the SD in the cancer group. Out of 82 benign samples, 39 samples had individual alanine concentrations overlapping with the concentrations detected in the cancer samples. If the cancer sample with the lowest alanine concentration is removed, then only six out of 82 overlapped. There was no significant difference ($P > 0.05$) between alanine levels in benign predominantly stromal (0.13 ± 0.05 mmol/kg, $N = 54$) or predominantly glandular (0.16 ± 0.06 mmol/kg, $N = 28$) prostate tissues.

The lactate and alanine concentrations observed in benign tissue samples were also separated according to the clinical diagnosis. A total of 44 prostate biopsies were from patients with a negative biopsy result, and 38 were from patients with a positive biopsy. No significant differences ($P > 0.05$) were observed for lactate (negative: 0.61 ± 0.28 mmol/kg vs. positive: 0.60 ± 0.29 mmol/kg) and alanine (negative: 0.14 ± 0.04 mmol/kg vs. positive: 0.15 ± 0.08 mmol/kg) concentrations between benign biopsies obtained from patients with and without a positive biopsy finding.

DISCUSSION

Healthy prostate tissue has been described as having a low rate of respiration, high anaerobic glycolysis, and considerable aerobic glycolysis (36,37). This is due to the unique function of healthy prostatic epithelial cells to synthesize and secrete large amounts of citrate rather than use it for energy production or lipogenesis (36,37). It has been proposed that this inefficient and low level of energy production is insufficient for cells to perform the synthetic and bioenergetic requirements that are essential for the growth and proliferation of prostate cancer (36,37). In general, cancer has been associated with an increase in glycolytic flux, and high lactate concentrations have been associated with more aggressive disease and metastasis while lower lactate concentrations have shown an overall longer and disease-free survival (38–41). The amino acid alanine is another important end-product of glucose utilization, which is required in cytosolic amino acid transformations and in protein synthesis (42). Alanine and citrate are also end-products of glutamate oxidation, which has been found to be a major source of respiratory energy in cancer

(42). It has been suggested that this alternative pathway is required to maintain lipogenesis/cholesterogenesis, which is especially needed for the formation of cellular membranes in proliferating cancer cells (36).

Because of the earlier detection and down-staging of prostate cancer that has occurred in recent years, new biomarkers are necessary to better identify and distinguish potentially aggressive cancers from those that are not as aggressive. In this study, lactate and alanine were investigated as potential biomarkers for prostate adenocarcinoma. ^{1}H HR-MAS spectroscopy provided high-quality spectra from TRUS-guided prostate biopsies, and the reference method ERETIC was robust for absolute quantification of lactate and alanine concentrations in intact biopsy tissue. Compared to previously reported lactate concentrations in surgical samples (~45 mmol/kg) (27), very low concentrations (<1.0 mmol/kg) were observed in benign prostate biopsies. This indicates that minimal anaerobic glycolysis occurs during biopsy collection (≤15 s), and biopsies therefore provide a better "snapshot" of in vivo metabolism. Additionally, the minimal changes in lactate (3.6%) and alanine (0.6%) during the experiments shows that biopsy tissues are well suited for studies on glycolysis.

The significant increase in lactate concentration found in prostate cancer biopsies is in agreement with previous studies of lactate in other human cancers (38–41). It was concluded that high lactate concentrations in solid tumors are not just a substitute for hypoxia, but a balance between a permanent generation of lactate and inefficient microcirculation in the tumor (41). This is explained by the "Warburg effect," where high lactate production is observed in malignant cells even in the presence of oxygen. An elevation in aerobic glycolysis might therefore be a fundamental property of cancer cells. Lactate has also been found to enhance the degree of tumor malignancy by activation of hyaluronan synthesis (43), upregulation of the growth factor VEGF (44), and the hypoxia-inducible factor HIF-1alpha (45). These mechanisms generate favorable conditions for metastatic spread. Thus, lactate accumulation in prostate cancer tissue may reflect the degree of tumor malignancy and may be related to the outcome of the disease. The isoenzymes of lactate dehydrogenase (LDH) catalyze the interconversion of lactate and pyruvate in the pathway of glycolysis. Several studies have shown that LDH is upregulated in other cancer types, such as ovarian cancer (46), colorectal cancer (47), and lung cancer (48). Therefore, an elevation in LDH levels in prostate cancer tissue might contribute to the elevated concentration of lactate.

The observation of significantly higher alanine concentrations in prostate cancer tissue supports the theory that tumor malignancy is associated with an increase in glycolytic flux, and is also consistent with the need for increased protein synthesis in tumors (36). Only a few previous studies have investigated alanine levels related to cancer, but the present results are in agreement with a study suggesting that glutamate oxidation may be a major source of respiratory energy for tumor cells (42). Glutamate is transaminated primarily to pyruvate to form alanine, and increased alanine concentrations may in this case be a result of the need for membranogenesis (lipogenesis) in proliferating cancer cells (36). Additionally, the transamination to alanine from pyruvate is catalyzed by the enzyme alanine transaminase (ALT); however, further studies are needed to establish the activity of ALT in prostate cancer tissue. The increase in alanine concentration could also be derived from catabolism of cellular proteins caused by the cancer. This study shows that alanine is an important biomarker in prostate cancer tissue, but further studies are needed to find the underlying biochemical pathways for alanine utilization in prostate cancer.

A growing amount of published data indicate that the metabolic information provided by MRSI combined with the anatomical information provided by MRI can significantly improve the clinical assessment of prostate cancer extent and location (1–6), extracapsular spread (7,8) and aggressiveness (9,10). The presence of thousands of whole-body 1.5T MRI scanners in hospitals worldwide and the availability of commercial MRI/MRSI packages will allow the routine clinical use of these techniques. Despite its value, combined MRI/MRSI has recognized limitations at 1.5T, including the potential for false-positive and false-negative results, particularly in patients with early-stage cancer (15). New biomarkers such as lactate and alanine could reduce the number of false-positives and -negatives in 1.5T MRI/MRSI studies of prostate cancer patients. In current commercial 1.5T MRI/MRSI packages, the lactate and alanine region of the spectrum is not excited to minimize periprostatic lipid contamination. However, with improved volume selection, outer voxel suppression techniques, and higher-field (3T) scanners, it is becoming feasible to use spectral-spatial RF editing sequences to detect lactate and alanine (21).

Additionally, new hyperpolarized ^{13}C MR techniques could potentially exploit lactate and alanine as biomarkers in future clinical investigations. Because of the unprecedented NMR signal enhancement (~50,000-fold) provided by hyperpolarized ^{13}C techniques, the transformation of pyruvate into lactate and alanine can be detected noninvasively in less than a minute (49), and the glycolytic status of the cell and the metabolic difference between normal and cancer tissue can therefore be quantified and mapped (49). Therefore, the changes in lactate and alanine observed in the present study could be used to improve the clinical diagnosis and characterization of human prostate cancer using lactate and alanine edited ^{1}H or hyperpolarized ^{13}C SI sequences.

Prostate cancer is found to have a broad range of biological malignancies, and histopathological heterogeneity-(both regional and cellular) is a challenge in characterizing the cancer and the different tumor grades. The Gleason scoring system evaluates this heterogeneity by scoring how effectively cancer cells are able to structure themselves into glands resembling those of the normal prostate. However, there are often discrepancies in pathologic scoring, and the present study is therefore based on average readings from two pathologists. For prostate biopsy tissue, there was good consensus among the pathology scores. Benign prostate tissue is also heterogeneous and confounding factors such as chronic inflammation (prostatitis) and BPH were accounted for in this study. By collecting larger numbers of samples, these confounding factors can potentially be separated by their metabolic patterns. In future studies, the concentrations of lactate and/or alanine

may be of importance as biomarkers for the diagnosis of these benign conditions. Likewise, metabolic studies of different prostate zones would be of interest in understanding regional metabolic and pathologic relationships.

There were a few notable limitations in the present study. Although biopsy tissues provided a more accurate snapshot of in vivo metabolism, there were an increased number of contaminants compared to surgical samples. These contaminants arose from periprostatic lipid contamination and the topical anesthetic (Hurricaine®; Beutlich) that was applied prior to the TRUS procedure. This resulted in 32 (~25%) of the biopsy samples being unusable in the current study. Additionally, only two samples could be obtained per patient and the sample sizes were much smaller than what can be obtained from surgical specimens. Finally, the relatively small number of biopsies containing cancer in this study, which is consistent with the down-staging of prostate cancer in the PSA era, limits our ability to assess changes in lactate and alanine concentration with cancer grade. Nevertheless, the use of biopsy tissues was critical for this study in order to minimize the impact of anaerobic glycolysis, which occurs in surgical specimens, on lactate and alanine concentrations.

In summary, using quantitative HR-MAS spectroscopy of snap-frozen prostate biopsies, it was determined that lactate and alanine concentrations were very low in benign prostate biopsy samples, and were significantly elevated in biopsy samples containing prostate cancer. The magnitude of elevation in the concentration of these metabolites is most likely a function of both the percentage of the biopsy core that is cancer and the pathologic grade of the cancer, but this will need to be determined in a study involving a larger number of malignant biopsies. The significant increase in the concentration of both lactate and alanine in biopsy samples containing as little as 5% cancer, and the minimal overlap of lactate concentrations between benign and malignant biopsies suggest that lactate and possibly alanine will be useful biomarkers that could be utilized in hyperpolarized ^{13}C MRSI staging exams of prostate cancer patients.

REFERENCES

1. Hasumi M, Suzuki K, Taketomi A, Matsui H, Yamamoto T, Ito K, Kurokawa K, Aoki J, Endo K, Yamanaka H. The combination of multivoxel MR spectroscopy with MR imaging improve the diagnostic accuracy for localization of prostate cancer. Anticancer Res 2003;23:4223–4227.
2. Portalez D, Malavaud B, Herigault G, Lhez JM, Elman B, Jonca F, Besse J, Pradere M. Predicting prostate cancer with dynamic endorectal coil MR and proton spectroscopic MR imaging. J Radiol 2004;85(12 Pt 1):1999–2004.
3. Scheidler J, Hricak H, Vigneron DB, Yu KK, Sokolov DL, Huang LR, Zaloudek CJ, Nelson SJ, Carroll PR, Kurhanewicz J. Prostate cancer: localization with three-dimensional proton MR spectroscopic imaging—clinicopathologic study. Radiology 1999;213:473–480.
4. Squillaci E, Manenti G, Mancino S, Carlani M, Di Roma M, Colangelo V, Simonetti G. MR spectroscopy of prostate cancer. Initial clinical experience. J Exp Clin Cancer Res 2005;24:523–530.
5. Wefer AE, Hricak H, Vigneron DB, Coakley FV, Lu Y, Wefer J, Mueller-Lisse U, Carroll PR, Kurhanewicz J. Sextant localization of prostate cancer: comparison of sextant biopsy, magnetic resonance imaging and magnetic resonance spectroscopic imaging with step section histology. J Urol 2000;164:400–404.
6. Vilanova JC, Barcelo J. Prostate cancer detection: magnetic resonance (MR) spectroscopic imaging [Review]. Abdom Imaging. 2007;32:253–261.
7. Yu KK, Scheidler J, Hricak H, Vigneron DB, Zaloudek CJ, Males RG, Nelson SJ, Carroll PR, Kurhanewicz J. Prostate cancer: prediction of extracapsular extension with endorectal MR imaging and three-dimensional proton MR spectroscopic imaging. Radiology 1999;213:481–488.
8. Wang L, Hricak H, Kattan MW, Chen HN, Scardino PT, Kuroiwa K. Prediction of organ-confined prostate cancer: incremental value of MR imaging and MR spectroscopic imaging to staging nomograms. Radiology 2006;238:597–603.
9. Kurhanewicz J, Vigneron DB, Males RG, Swanson MG, Yu KK, Hricak H. The prostate: MR imaging and spectroscopy. Present and future. Radiol Clin North Am 2000;38:115–138, viii–ix.
10. Zakian KL, Sircar K, Hricak H, Chen HN, Shukla-Dave A, Eberhardt S, Muruganandham M, Ebora L, Kattan MW, Reuter VE, Scardino PT, Koutcher JA. Correlation of proton MR spectroscopic imaging with gleason score based on step-section pathologic analysis after radical prostatectomy. Radiology 2005;234:804–814.
11. Coakley FV, Teh HS, Qayyum A, Swanson MG, Lu Y, Roach M, Pickett B, Shinohara K, Vigneron DB, Kurhanewicz J. Endorectal MR imaging MR spectroscopic imaging for locally recurrent prostate cancer after external beam radiation therapy: preliminary experience. Radiology 2004;233:441–448.
12. Mueller-Lisse UG, Swanson MG, Vigneron DB, Hricak H, Bessette A, Males RG, Wood PJ, Noworolski S, Nelson SJ, Barken I, Carroll PR, Kurhanewicz J. Time-dependent effects of hormone-deprivation therapy on prostate metabolism as detected by combined magnetic resonance imaging and 3D magnetic resonance spectroscopic imaging. Magn Reson Med 2001;46:49–57.
13. Mueller-Lisse UG, Vigneron DB, Hricak H, Swanson MG, Carroll PR, Bessette A, Scheidler J, Srivastava A, Males RG, Cha I, Kurhanewicz J. Localized prostate cancer: Effect of hormone deprivation therapy measured by using combined three-dimensional H-1 MR spectroscopy and MR imaging: clinicopathologic case-controlled study. Radiology 2001; 221:380–390.
14. Ryan CJ, Small EJ. Prostate cancer update: 2005. Curr Opin Oncol 2006;18:284–288.
15. Hricak H, Choyke PL, Eberhardt SC, Leibel SA, Scardino PT. Imaging prostate cancer: a multidisciplinary perspective. Radiology 2007;243: 28–53.
16. Nelson SJ, Vigneron DB, Star-Lack J, Kurhanewicz J. High spatial resolution and speed in MRSI. NMR Biomed 1997;10:411–422.
17. Ardenkjaer-Larsen JH, Fridlund B, Gram A, Hansson G, Hansson L, Lerche MH, Servin R, Thaning M, Golman K. Increase in signal-to-noise ratio of >10,000 times in liquid-state NMR. Proc Natl Acad Sci USA 2003;100:10158–10163.
18. Chen AP, Albers MJ, Cunningham CH, Kohler SJ, Yen YF, Hurd RE, Tropp J, Bok R, Pauly JM, Nelson SJ, Kurhanewicz J, Vigneron DB. Hyperpolarized C-13 spectroscopic imaging of the TRAMP mouse at 3T—initial experience. Magn Reson Med 2007;58:1099–1106.
19. Kohler SJ, Yen Y, Wolber J, Chen AP, Albers MJ, Bok R, Zhang V, Tropp J, Nelson SJ, Vigneron DB, Kurhanewicz J, Hurd RE. In vivo 13-carbon metabolic imaging at 3T with hyperpolarized 13C-1-pyruvate. Magn Reson Med 2007;58:65–69.
20. Star-Lack J, Spielman D, Adalsteinsson E, Kurhanewicz J, Terris DJ, Vigneron DB. In vivo lactate editing with simultaneous detection of choline, creatine, NAA, and lipid singlets at 1.5 T using PRESS excitation with applications to the study of brain and head and neck tumors. J Magn Reson 1998;133:243–254.
21. Cunningham CH, Vigneron DB, Chen AP, Xu D, Hurd RE, Sailasuta N, Pauly JM. Design of symmetric-sweep spectral-spatial RF pulses for spectral editing. Magn Reson Med 2004;52:147–153.
22. Gingrich JR, Barrios RJ, Morton RA, Boyce BF, DeMayo FJ, Finegold MJ, Angelopoulou R, Rosen JM, Greenberg NM. Metastatic prostate cancer in a transgenic mouse. Cancer Res 1996;56:4096–4102.
23. Cooper JF, Farid I. The role of citric acid in the physiology of the prostate. 3. Lactate/citrate ratios in benign and malignant prostatic homogenates as an index of prostatic malignancy. J Urol 1964;92:533–536.
24. Cornel EB, Smits GA, Oosterhof GO, Karthaus HF, Deburyne FM, Schalken JA, Heerschap A. Characterization of human prostate cancer, benign prostatic hyperplasia and normal prostate by in vitro 1H and 31P magnetic resonance spectroscopy. J Urol 1993;150:2019–2024.
25. Yacoe ME, Sommer G, Peehl D. In vitro proton spectroscopy of normal and abnormal prostate. Magn Reson Med 1991;19:429–438.

26. Schiebler ML, Miyamoto KK, White M, Maygarden SJ, Mohler JL. In vitro high resolution 1H-spectroscopy of the human prostate: benign prostatic hyperplasia, normal peripheral zone and adenocarcinoma. Magn Reson Med 1993;29:285–291.
27. Swanson MG, Zektzer AS, Tabatabai ZL, Simko J, Jarso S, Keshari KR, Schmitt L, Carroll PR, Shinohara K, Vigneron DB, Kurhanewicz J. Quantitative analysis of prostate metabolites using 1H HR-MAS spectroscopy. Magn Reson Med 2006;55:1257–1264.
28. Akoka S, Trierweiler M. Improvement of the ERETIC method by digital synthesis of the signal and addition of a broadband antenna inside the NMR probe. Instrum Sci Technol 2002;30:21–29.
29. Akoka S, Barantin L, Trierweiler M. Concentration measurement by proton NMR using the ERETIC method. Anal Chem 1999;71:2554–2557.
30. Meiboom S, Gill D. Modified spin-echo method for measuring nuclear relaxation times. Rev Sci Instrum 1958;29:688–691.
31. Ziarelli F, Caldarelli S. Solid-state NMR as an analytical tool: quantitative aspects. Solid State Nucl Magn Reson 2006;29:214–218.
32. Zektzer AS, Swanson MG, Jarso S, Nelson SJ, Vigneron DB, Kurhanewicz J. Improved signal to noise in high-resolution magic angle spinning total correlation spectroscopy studies of prostate tissues using rotor-synchronized adiabatic pulses. Magn Reson Med 2005;53:41–48.
33. Diggle PJ Liang K-Y, Zeger SL. Analysis of longitudinal data. Oxford University Press: New York; 1994. p 78–116.
34. Cheng LL, Wu C, Smith MR, Gonzalez RG. Non-destructive quantitation of spermine in human prostate tissue samples using HRMAS 1H NMR spectroscopy at 9.4 T. FEBS Lett 2001;494:112–116.
35. Swanson MG, Vigneron DB, Tabatabai ZL, Males RG, Schmitt L, Carroll PR, James JK, Hurd RE, Kurhanewicz J. Proton HR-MAS spectroscopy and quantitative pathologic analysis of MRI/3D-MRSI-targeted postsurgical prostate tissues. Magn Reson Med 2003;50:944–954.
36. Costello LC, Franklin RB. 'Why do tumour cells glycolyse?': from glycolysis through citrate to lipogenesis. Mol Cell Biochem 2005;280:1–8.
37. Costello LC, Franklin RB. Bioenergetic theory of prostate malignancy. Prostate 1994;25:162–166.
38. Brizel DM, Schroeder T, Scher RL, Walenta S, Clough RW, Dewhirst MW, Mueller-Klieser W. Elevated tumor lactate concentrations predict for an increased risk of metastases in head-and-neck cancer. Int J Radiat Oncol Biol Phys 2001;51:349–353.
39. Schwickert G, Walenta S, Sundfor K, Rofstad EK, Mueller-Klieser W. Correlation of high lactate levels in human cervical cancer with incidence of metastasis. Cancer Res 1995;55:4757–4759.
40. Walenta S, Chau TV, Schroeder T, Lehr HA, Kunz-Schughart LA, Fuerst A, Mueller-Klieser W. Metabolic classification of human rectal adenocarcinomas: a novel guideline for clinical oncologists? J Cancer Res Clin Oncol 2003;129:321–326.
41. Walenta S, Schroeder T, Mueller-Klieser W. Lactate in solid malignant tumors: potential basis of a metabolic classification in clinical oncology. Curr Med Chem 2004;11:2195–2204.
42. Moreadith RW, Lehninger AL. The pathways of glutamate and glutamine oxidation by tumor cell mitochondria. Role of mitochondrial NAD(P)+-dependent malic enzyme. J Biol Chem 1984;259:6215–6221.
43. Rudrabhatla SR, Mahaffey CL, Mummert ME. Tumor microenvironment modulates hyaluronan expression: the lactate effect. J Invest Dermatol 2006;126:1378–1387.
44. Delongchamps NB, Peyromaure M, Dinh-Xuan AT. Role of vascular endothelial growth factor in prostate cancer. Urology 2006;68:244–248.
45. Kimbro KS, Simons JW. Hypoxia-inducible factor-1 in human breast and prostate cancer. Endocr Relat Cancer 2006;13:739–749.
46. Schneider D, Halperin R, Langer R, Bukovsky I, Herman A. Peritoneal fluid lactate dehydrogenase in ovarian cancer. Gynecol Oncol 1997;66:399–404.
47. Koukourakis MI, Giatromanolaki A, Simopoulos C, Polychronidis A, Sivridis E. Lactate dehydrogenase 5 (LDH5) relates to up-regulated hypoxia inducible factor pathway and metastasis in colorectal cancer. Clin Exp Metastasis 2005;22:25–30.
48. Chen Y, Zhang H, Xu A, Li N, Liu J, Liu C, Lv D, Wu S, Huang L, Yang S, He D, Xiao X. Elevation of serum l-lactate dehydrogenase B correlated with the clinical stage of lung cancer. Lung Cancer 2006;54:95–102.
49. Golman K, Zandt RI, Lerche M, Pehrson R, Ardenkjaer-Larsen JH. Metabolic imaging by hyperpolarized 13C magnetic resonance imaging for in vivo tumor diagnosis. Cancer Res 2006;66:10855–10860.